AIP | Review of Scientific Instruments

Honeycomblike large area LaB6 plasma source for Multi-Purpose Plasma facility

Hyun-Jong Woo, Kyu-Sun Chung, Hyun-Jong You, Myoung-Jae Lee, Taihyeop Lho et al.

Citation: Rev. Sci. Instrum. **78**, 103505 (2007); doi: 10.1063/1.2794705
View online: http://dx.doi.org/10.1063/1.2794705
View Table of Contents: http://rsi.aip.org/resource/1/RSINAK/v78/i10
Published by the American Institute of Physics.

Honeycomblike large area LaB_6 plasma source for Multi-Purpose Plasma facility

Hyun-Jong Woo, Kyu-Sun Chung, Hyun-Jong You, and Myoung-Jae Lee[a)]
electric Probe Applications Laboratory (ePAL), Hanyang University, Seoul 133-791, Korea

Taihyeop Lho, Kwon Kook Choh, Jung-Sik Yoon, Yong Ho Jung, Bongju Lee, Suk Jae Yoo, and Myeon Kwon
National Fusion Research Institute, Daejeon 305-333, Korea

(Received 1 May 2007; accepted 14 September 2007; published online 15 October 2007)

A Multi-Purpose Plasma (MP^2) facility has been renovated from Hanbit mirror device [Kwon *et al.*, Nucl. Fusion **43**, 686 (2003)] by adopting the same philosophy of diversified plasma simulator (DiPS) [Chung *et al.*, Contrib. Plasma Phys. **46**, 354 (2006)] by installing two plasma sources: LaB_6 (dc) and helicon (rf) plasma sources; and making three distinct simulators: divertor plasma simulator, space propulsion simulator, and astrophysics simulator. During the first renovation stage, a honeycomblike large area LaB_6 (HLA-LaB_6) cathode was developed for the divertor plasma simulator to improve the resistance against the thermal shock fragility for large and high density plasma generation. A HLA-LaB_6 cathode is composed of the one inner cathode with 4 in. diameter and the six outer cathodes with 2 in. diameter along with separate graphite heaters. The first plasma is generated with Ar gas and its properties are measured by the electric probes with various discharge currents and magnetic field configurations. Plasma density at the middle of central cell reaches up to 2.6×10^{12} cm^{-3}, while the electron temperature remains around 3–3.5 eV at the low discharge current of less than 45 A, and the magnetic field intensity of 870 G. Unique features of electric property of heaters, plasma density profiles, is explained comparing with those of single LaB_6 cathode with 4 in. diameter in DiPS. © *2007 American Institute of Physics.*
[DOI: 10.1063/1.2794705]

I. INTRODUCTION

Hanbit mirror device[1] was renovated as a Multi-Purpose Plasma (MP^2) facility for the divertor plasma simulation, space propulsion, and astrophysical researches with two plasma sources—LaB_6 (dc) and helicon (rf) plasmas—to be installed through the three renovation stages (3 years per stage). The research objectives of the MP^2 are the following.

(i) Divertor plasma simulation (basically with LaB_6 plasma source), such as liquid divertor experiments with molten-salt target[2] and gas puffing experiments,[3,4] planned at the first renovation stage.
(ii) Space propulsion experiments (basically with helicon plasma source), such as current-free double layer formation,[5] ion cyclotron range of frequency (ICRF) heating effect on the specific impulse,[6,7] and plasma detachment from the magnetic field line,[8] will be started at second renovation stage.
(iii) Astrophysical researches, such as magnetic reconnection experiment[9,10] and Alfven wave studies,[11] will be started at third renovation stage.

Although the basic design concept of MP^2 is adopted from the DiPS,[12] the MP^2 has unique features such as (i) the largest LaB_6 cathode, (ii) two magnetic field regions—high field (>3 kG) with simple mirror regions, and (iii) flexibility for future space/astrophysical experiment with helicon source, large space, and various diagnostics as a national plasma user facility in Korea. The MP^2 will carry its own experiments relating future fusion divertor science, yet it will be open to users depending on their proposal with provision of large spectrum of plasma parameters: (i) source type (dc and rf), (ii) plasma size (>25 cm diameters), (iii) density (10^6–10^{13} cm^{-3}), (iv) electron temperature (0.1–10 eV), and (v) magnetic field (0–3 kG) along with various diagnostics (electric probes, microwave interferometer, laser Thomson scattering, optical emission spectroscopy, etc). During the first renovation stage, the divertor plasma simulator was developed with the LaB_6 plasma source. Since the LaB_6 has a high thermal electron emission rate, low evaporation rate, and high resistance to contamination in vacuum break, the LaB_6 cathode has been used for plasma generation in many divertor plasma simulators such as PISCES A[13] and B,[14] PSI-II,[15] NAGDIS-II,[16] TPD-IV,[17] MAP-II,[18] and DiPS.[12] However, the LaB_6 plate can be easily broken due to the weakness against the thermal shock, making it difficult to manufacture the large area LaB_6 cathode (larger than 15 cm in diameter) with one LaB_6 plate.[13] The thermal stress on the LaB_6 originates by a sudden temporal variation and by the nonuniformity of the temperature on the LaB_6 surface. The temporal variations of the temperature take place during the rapid heating of LaB_6 and the current overflow in a flash on the LaB_6 surface. These are easily overcome by slow in-

a)FAX: +82-2-2299-1908. Electronic mail: mjlee@hanyang.ac.kr

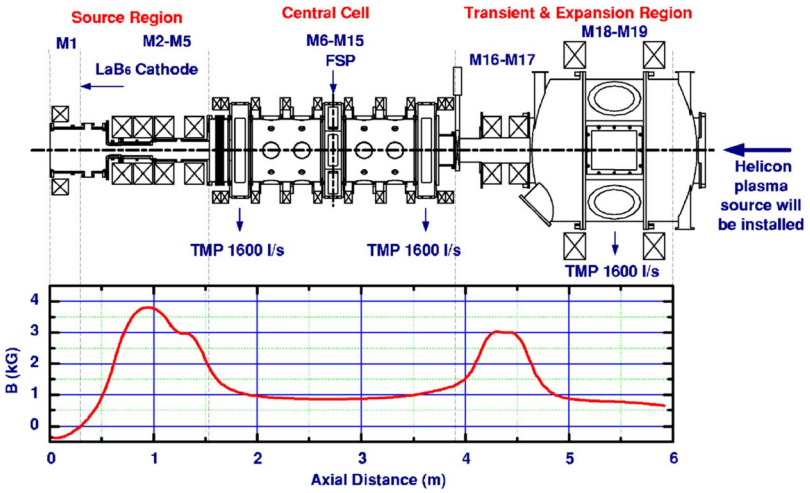

FIG. 1. (Color online) Schematic diagram of Multi-Purpose Plasma (MP^2) facility and its magnetic field intensity profile (MF2).

crease of the heater power and by use of the discharge power supply with good feedback control. The nonuniformity of temperature is due to the nonuniform heating of LaB_6 cathode by the external heaters and concentrations of heat fluxes by plasma, especially ions, on small portions of LaB_6 surface. These are hard to be overcome when using one large LaB_6 plate. However, it can be mitigated by applying uniform heating using a larger heaters than LaB_6 size or by spreading the heat from plasma, making the null point with cusp magnetic field.

To increase the lifetime of LaB_6 by reducing the thermal stress on the LaB_6 surface, the honeycomblike large area LaB_6 (HLA-LaB_6) cathode was developed by installing a multiple array of LaB_6 plates with a smaller diameter. Thermal stress caused by the steep gradient of thermal resistance can be reduced by having the uniform thermal expansion rate, which can be achieved by making uniform temperature distribution in smaller LaB_6 plates. In addition, one can easily expand the cathode size and operates the HLA-LaB_6 cathode since it does not have the matching problems such as the multiarrays of helicon sources.[19]

In this paper, the design parameters of divertor plasma simulator of MP^2 and the HLA-LaB_6 cathode are introduced with the initial Ar plasma parameters measured by a single probe installed on a fast scanning system. Its initial plasma parameters and electric property of cathode are compared with those of single LaB_6 cathode as in DiPS.[12]

II. EXPERIMENTAL SETUP

A large scale divertor simulator (6.3 m long and 0.6 m diameter) of MP^2 has been developed for divertor and edge plasmas and plasma-material interactions during the first renovation stage. Figure 1 shows the schematic diagram and magnetic intensity profile of MP^2, especially the divertor plasma simulator. The divertor plasma simulator is composed of plasma source region, central cell region, and expansion region. The divertor plasma simulator of MP^2 has 19 electromagnets, which are numbered as M1–M19 started from the LaB_6 cathode. The first plasma is generated with Ar gas in the following conditions.

(i) Two magnetic field conditions of MF1 [−150 A (M1), 200 A (M2-M5, M16-M19), 350 A (M6-M15)] and MF2 [−300 A (M1), 400 A (M2-M5, M16-M19), 700 A (M6-M15)], where the minus sign indicates the opposite direction of the coil current for the generation of cusp field in the source region.
(ii) Neutral pressures of 30 mTorr (at source chamber) and 2.5 mTorr (at central cell).
(iii) Discharge voltages of 60–65 V and discharge currents of 5–45 A, which will be increased up to 400 A successively.
(iv) LaB_6 heating powers of 3.69 kW (250 A–14.74 V) for inner heater and 14.79 kW (390 A–37.9 V) for outer heater.

For the steady-state operation, one adopts MF2 field configuration as a maximum magnetic field, which is lower than that of previous Hanbit mirror device by 10%–20%, while keeping the temperature variation as 20 °C between inlet and outlet of cooling water during 4 h of operation.

Figure 2 shows the schematic diagram and magnetic field profile of the source region, which is composed of source chamber, floating electrode, anode, and high field

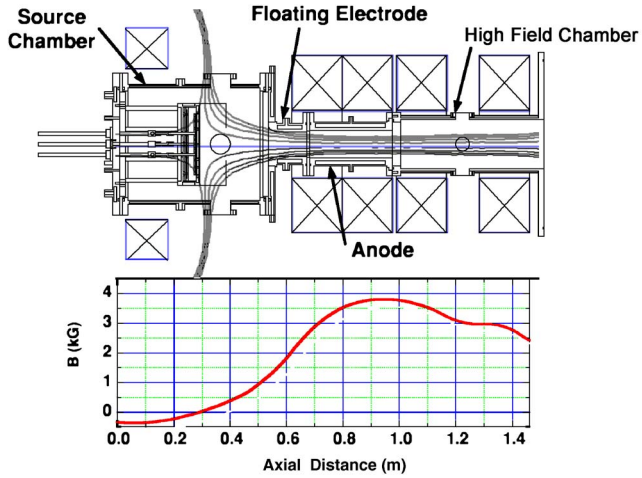

FIG. 2. (Color online) Schematic diagram of the source and high field region of the divertor plasma simulator in Multi-Purpose Plasma (MP^2) facility.

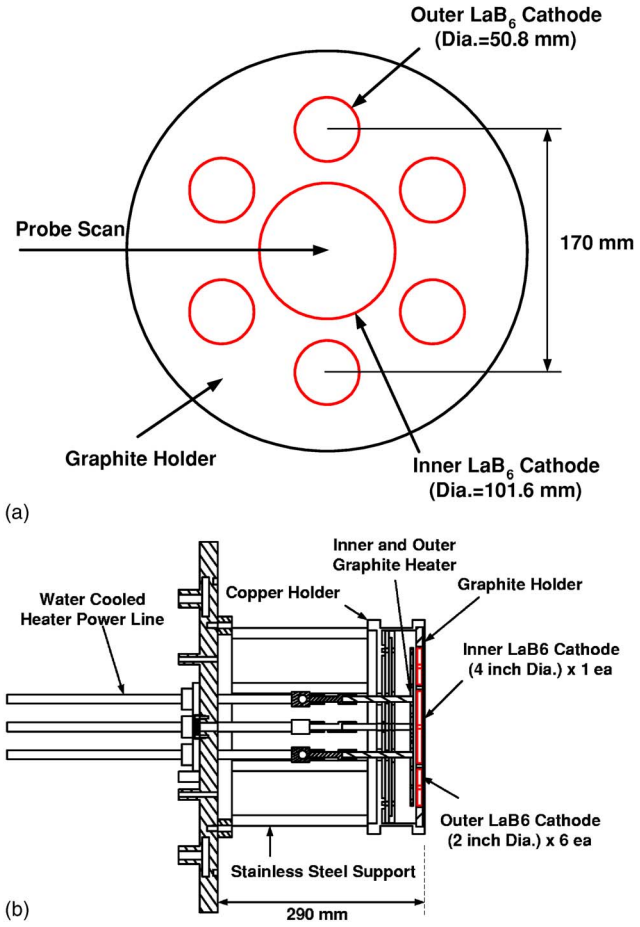

FIG. 3. (Color online) Schematic diagram of the honeycomblike large area LaB_6 cathode; (a) top view and (b) side view.

chamber. In this region, all the components have the double wall configuration to prevent the vacuum break from the high heating powers for LaB_6 cathode and high density plasma. The dimensions of the source chamber, floating electrode, anode, and high field chamber are 412 mm [inner diameter (ID)] $\times$520 mm [length (L)], 90 mm (ID) $\times$140 mm (L), 100 mm (ID)$\times$300 mm (L), and 180 mm (ID)$\times$550 mm (L), respectively. Teflon insulators with thickness of 10 mm are located between source flange and source chamber, source chamber and floating electrode, and floating electrode and anode for electrical insulation. The floating electrode plays a role as a buffer for reducing fluctuation of the electric field between LaB_6 cathode and anode caused by an abrupt current overflowing. The HLA-LaB_6 cathode surface is located at the null point (or minimum B) of the cusp magnetic field configuration for generating the high density plasma by focusing the electrons toward the anode and for reducing the thermal stresses on LaB_6 surface from ion bombardment heating by diverging the ions with magnetic field lines.

Figure 3 shows the schematic structure of HLA-LaB_6 cathode. As shown in Fig. 3(a), the HLA-LaB_6 is composed of one inner LaB_6 cathode with 4 in. diameter and six outer LaB_6 cathodes with 2 in. diameter. The LaB_6 cathode arrays are heated separately by inner and outer graphite heaters. Advantage of the graphite heater and other design are given in the previous work in detail.[12,20]

For analyzing plasma, MP^2 has the four diagnostic tools.

(i) Electric probes: fixed probe arrays, which are to be used as a single, double, and triple probes, and fast-scanning probe (FSP), where single and Mach probes are to be installed for the measurement of electron temperature, plasma density, plasma floating potential, and flow velocity.
(ii) Laser Thomson scattering (LTS) system with neodymium doped yttrium aluminum garnet laser (1 J at 532 nm, 10 Hz repetition rate) for the measurements of electron temperature and electron density.
(iii) Microwave interferometer (MI) with 8 GHz of cutoff frequency for the measurements of line integrated electron density and its fluctuation.
(iv) Optical emission spectroscopy with 1.3 m focal length for the measurements of electron density and temperature.

However, the LTS and MI are necessary to be modified for MP^2 plasmas ($<$20 eV of electron temperature and 10^{12}–10^{13} cm^{-3} of plasma density). The optical emission spectroscopy is also necessary to be modified, especially the fiber arrays for MP^2 plasma condition. Then, the radial profiles of plasma density and electron temperature are measured only by a single probe with 0.5 mm (diameter) and 4 mm (length), which is installed on the fast-scanning probe system at the middle of central cell.

III. RESULTS AND ANALYSIS

Figure 4(a) shows the saturated electrical resistance of the graphite heaters at each step of heating current versus the LaB_6 heating power (or heating current) applied to be HLA-LaB_6 cathodes, while Fig. 4(b) shows the normalized resistances, where the reference resistance R_0 is the value at 10 A of heating current. For the first plasma generation, the heating currents of inner and outer heaters are ramped up to 250 A for inner heater and 390 A for outer heater simultaneously for 1 h. The temperature of each heater can be estimated by the variations of the normalized resistance in Fig. 4(b) from the relationship between specific resistance of graphite and its temperature of Noyes.[21] The variation of the resistance, as shown in Fig. 4(a), is similar shape in both inner and outer heaters. Although that of outer heater is larger than inner heater due to geometrical length, its minimum values are obtained at almost same heating current, i.e., $\sim$110 A. From the variation of the normalized resistance (R/R_0), as shown in Fig. 4(b), the minimum values of all three heaters are obtained at similar heating power range, i.e., 0.5–1 kW. Two heaters are for the MP^2 and one is for DiPS. The inner heater of MP^2 has the same as that of DiPS. The normalized resistances of DiPS's heater and the outer heater of MP^2 are almost same ($\sim$0.77), while that of inner heater of MP^2 is a little bit larger, i.e., $\sim$0.8. This indicates that the temperature of the inner heater with the outer heater is higher than without the outer heater due to the additional heating from outer to inner by the concentric arrangement. However, the outer heater does not show the increase of temperature even with the inflow of heat from the inner

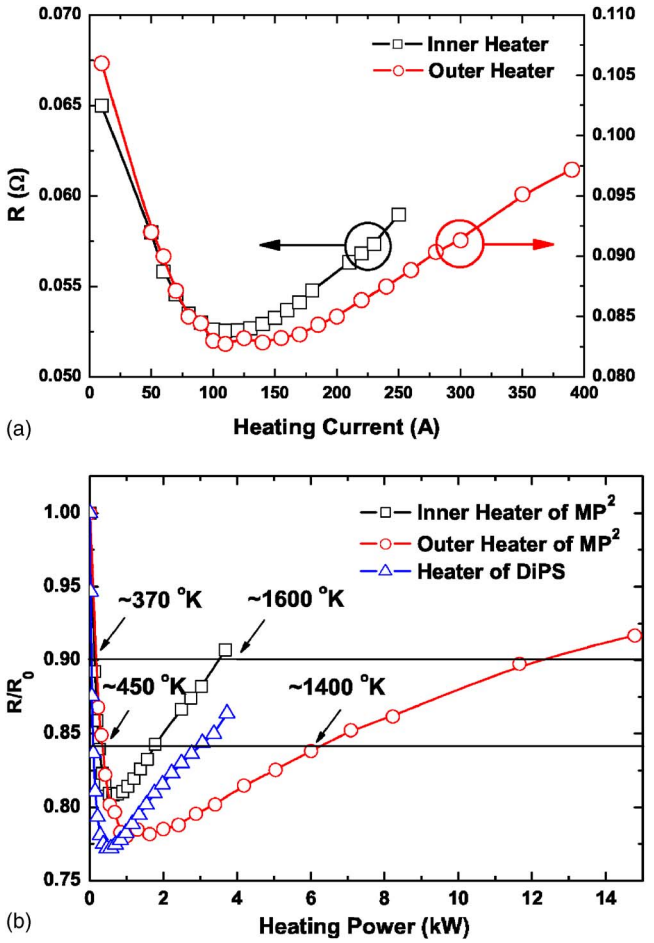

FIG. 4. (Color online) Graphite heater resistances; (a) heater resistances in terms of heating currents; (b) normalized heater resistance to the heater resistances [$R_0=R(10\ \mathrm{A})$].

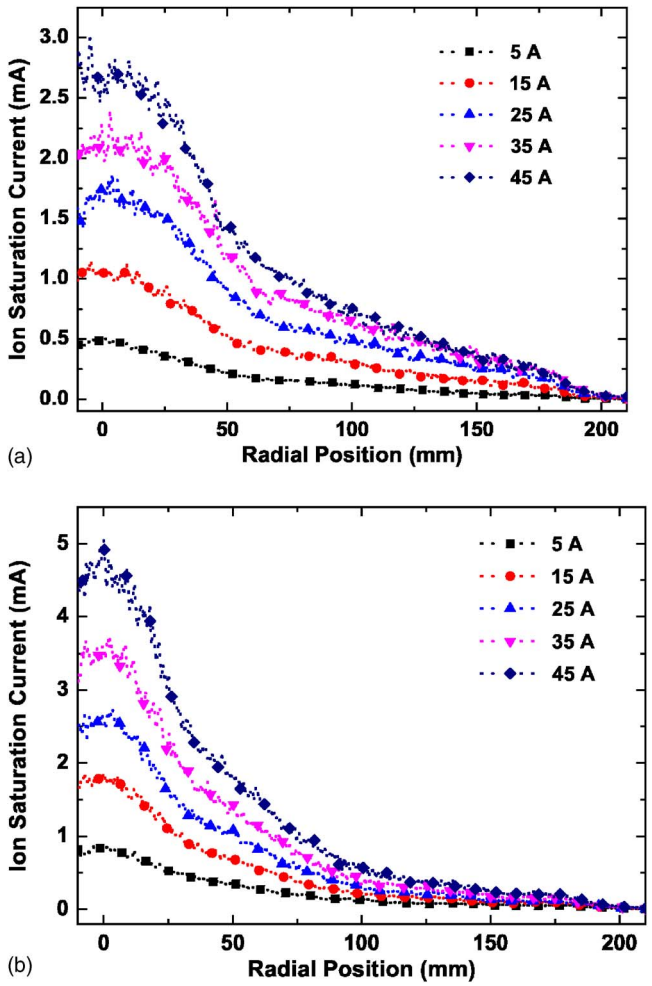

FIG. 5. (Color online) Ion saturation current profiles with different discharge currents at two magnetic fields; (a) MF 1: 435 G at measurement position and (b) MF 2: 870 G at measurement position.

heater. This increase might be either due to increase of heat loss to the wall with larger surface or due to the large volume ratio (or heat reservoir) of outer to inner heater, which is about 3.4. According to Fig. 4, it is possible to apply the heating powers up to 6 kW for inner heater and 25 kW for outer heater within the limits of the power supplies of 6.6 kW (20 V–330 A) and 30 kW (50 V–600 A), respectively.

Figure 5 shows the radial distributions of ion saturation currents with the discharge currents from 5 to 45 A at two magnetic field configurations of MF1 and MF2. The magnetic field intensities are 435 and 870 G at the scanning position ("FSP" in Fig. 1) in the two magnetic field configurations of MF1 and MF2, respectively. The half- and e-folding lengths, which represents the size of plasma column, are 52 mm (MF1) and 35 mm (MF2) and 78 mm (MF1) and 55 mm (MF2), respectively. Normalized ion saturation currents of MP^2 and DiPS are shown in Fig. 6(a). The ion saturation currents are normalized by the ion saturation currents at plasma center, I_0, and the radial position is also normalized by the plasma size, $r_{\mathrm{edge}} \equiv r(I/I_0=0.03)$, which is defined as the plasma edge for our convenience. In the low field regime (<500 G), they have similar profiles of radial ion saturation currents between HLA-LaB_6 cathode of MP^2 and single LaB_6 of DiPS. In the high field regime (~1000 G), however, the steepness of ion saturation current profile of HLA-LaB_6 cathode has been observed to be milder than that of DiPS for $r/r_{\mathrm{edge}} \geqslant 0.12$ (or 22 mm of the radial position). This might be caused by spatial localizations of the outer LaB_6 cathode contributions by decreasing the cross-field diffusion with magnetic field intensity, although they have same magnetic flux profiles. Although plasma generation with only the inner cathode is not performed in MP^2, one can expect that it may be similar profiles of ion saturation currents in MP^2 and DiPS since the size of LaB_6 plate and its geometrical scheme are almost the same. Hence, the differences of the normalized ion saturation current between HLA-LaB_6 and single LaB_6 cathodes are the contributions of ion saturation current (or plasma density) generated by the outer cathodes in MP^2. Since the diffusion coefficient is proportional to the $n/\nabla n$ with constant or slowly varying electron temperature spatially, the plasmas by the outer cathode seem to be more effectively diffused to the outer direction than the inner direction. Figures 6 and 7 show the classical confirmation of better confinement of plasmas due to high magnetic pressure. Radial profiles of density and electron temperature measured by a fast scanning single probe are shown in Fig. 7 at MF1 field configuration and in Fig. 8 at MF2 field configuration. At the plasma center, plasma densi-

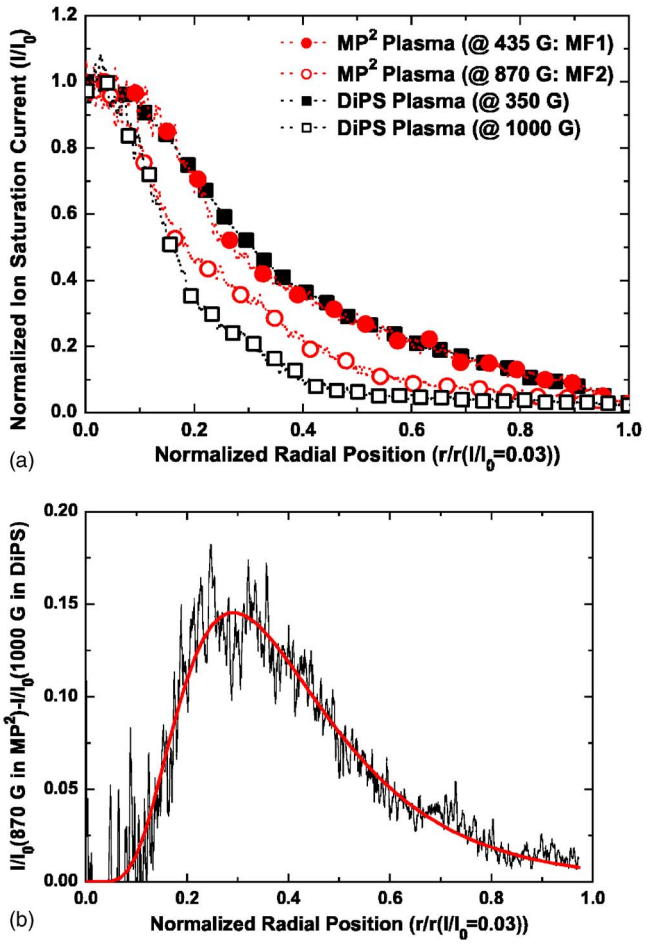

FIG. 6. (Color online) Normalized ion saturation current profiles of 45 A discharge currents. (a) Ion saturation current profile of MP^2 and DiPS plasmas and (b) difference of normalized current profile between MP^2 and DiPS in high field configuration: 870 G in MP^2 and 1000 G in DiPS.

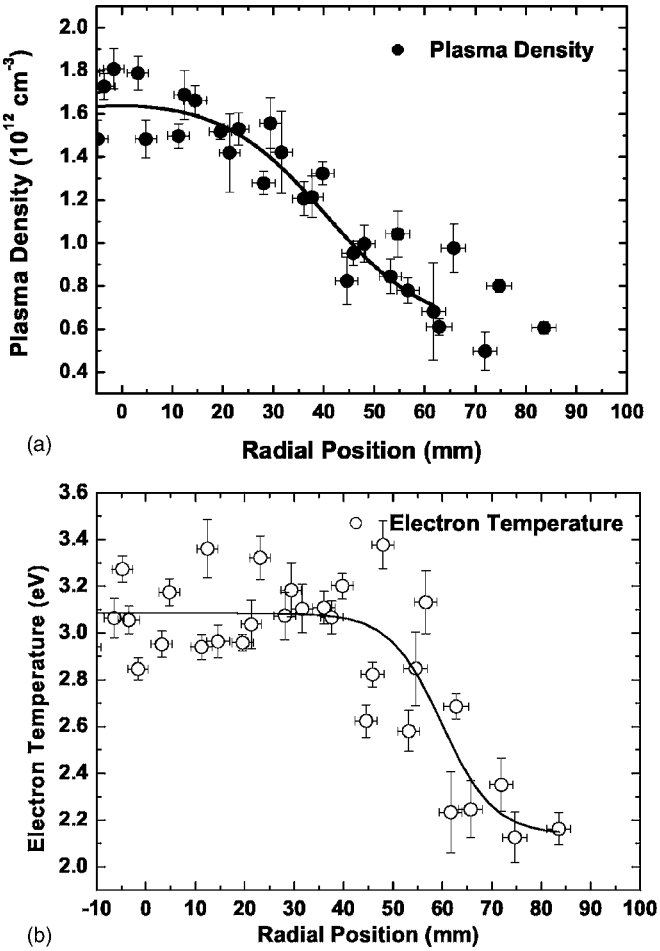

FIG. 7. Plasma density and electron temperature profiles measured at MF1 magnetic field configuration (a) plasma density and (b) electron temperature.

ties and electron temperatures are 1.6×10^{12} cm^{-3} and 3.1 eV at MF1 and 2.6×10^{12} cm^{-3} and 3.4 eV at MF2, respectively. The plasma densities are monotonically decreased radially, but the electron temperatures seem to be almost constant within the radii of 40 mm (MF1) and 15 mm (MF2). In lower magnetic field, the heating or generation of plasmas by the outer cathode along with inner cathode can contribute flattening the profiles of electron temperatures, compared with those by single LaB_6 cathode as in DiPS, even if it does not show in ion saturation current profile.[22]

Figure 9 shows the linear dependence of ion saturation currents upon the discharge current at the plasma center. This seems to confirm that the discharge voltage mainly affects the electron temperature, while the discharge current does the plasma density. As for the operation of the LaB_6 cathode, the discharge voltage would stay almost constant if sufficient electrons are emitted from the surface of LaB_6, i.e., it is possible to keep the discharge voltage as constant with fixed discharge current since there is an additional heating of the LaB_6 by ion bombardment, which can produce extra electrons necessary for higher discharge current operation while maintaining the heating powers of the external heaters as same. Hence, one can expect that the plasma densities can be increased linearly with the discharge current, which has also been observed in NAGDIS-II.[16] From Figs. 7–9, the plasma densities at center can be estimated to reach up to 1.3×10^{13} cm^{-3} at MF1 field configuration and 2.2×10^{13} cm^{-3} with MF2 field configuration at the 400 A of discharge currents. Future target value of discharge current of HLA-LaB_6 would be 400 A.

IV. SUMMARY

For Multi-Purpose Plasma (MP^2) facility, a divertor plasma simulator has been developed with honeycomblike large area LaB_6 (HLA-LaB_6) cathode for divertor and edge plasmas and plasma-material interactions. Electric properties of two cathodes of MP^2 are characterized by comparing the resistance of MP^2 with that of single LaB_6 cathode of DiPS. The initial plasma parameters are measured by a fast-scanning single probe at the middle of central cell. The large area and high density plasma is easily achieved by controlling the magnetic field configuration and discharge currents while overcoming the thermal shock problems on LaB_6 plate by multiple array. However, the density and temperature profiles of HLA-LaB_6 cathode are not similar to that of single LaB_6 cathode. In the high magnetic field configuration (MF2 configuration), it is clearly shown that the outer LaB_6 cathode contribute to build up the plasma density from radial profiles of the ion saturation currents in Figs. 5 and 6

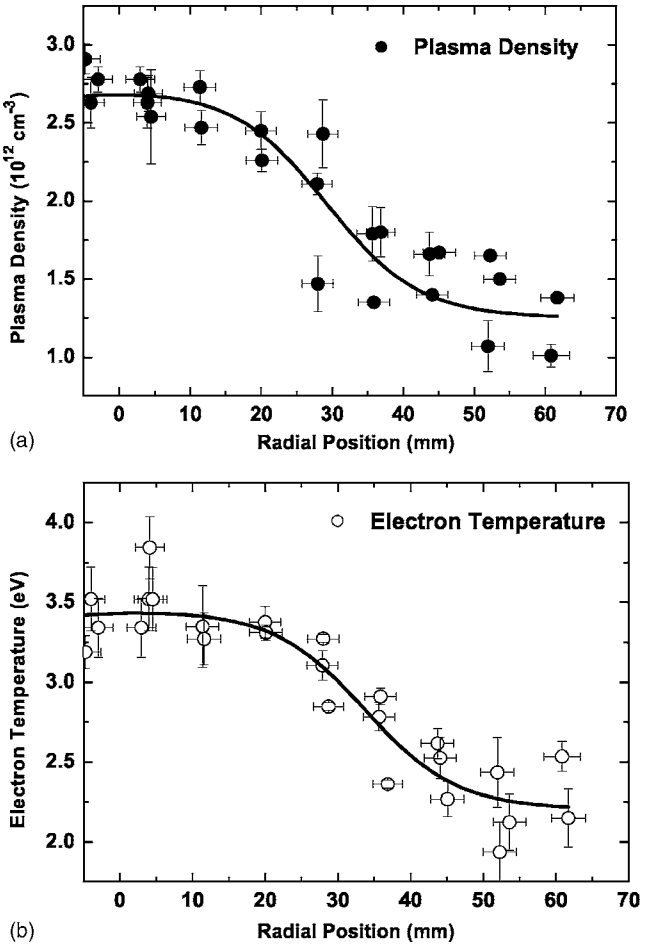

FIG. 8. Plasma density and electron temperature profiles measured at MF2 magnetic field configuration (a) plasma density and (b) electron temperature.

by shrinking the cross-field diffusion. Although contributions of the outer cathode are not clearly shown in the ion saturation current profiles at low field regime (MF1 configuration), one can expect that it is a combined effect of both the inner and outer cathodes from flat electron temperatures. The measured plasma densities are reached up to 1.6×10^{12} cm^{-3} at 435 G (MF1 configuration) and 2.6×10^{12} cm^{-3} at 870 G (MF2 configuration), while the electron temperatures remain about 3.2 ± 0.2 eV at 45 A of discharge currents. If one increases the discharge current up to 400 A, the maximum plasma densities are to be estimated as 1.3×10^{13} cm^{-3} at MF1 configuration and 2.2×10^{13} cm^{-3} at MF2 configuration with Ar gas based on the linearity of ion saturation current to the discharge current shown in Fig. 9. Optimization of HLA-LaB_6 plasmas is provided as an aid to future experiments with heater powers for inner and outer LaB_6 cathodes (or its ratios), discharge currents (up to 100 A), magnetic field configurations, and the gas types (Ar, He, and H_2).

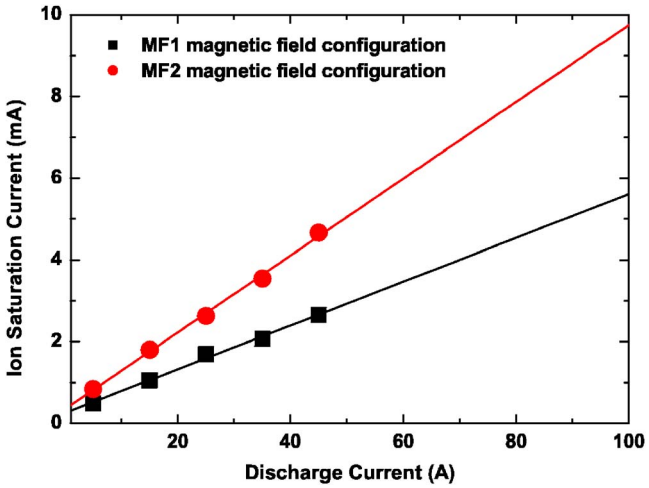

FIG. 9. (Color online) Ion saturation current variation with the discharge current at the plasma center.

ACKNOWLEDGMENTS

This work is supported partially by the Hanbit User Program of National Fusion Research Institute (NFRI: formerly Korea Basic Science Institute) and partially by the National Research Laboratory (NRL) program of the Korea Science and Engineering Foundation (KOSEF) under the Ministry of Science and Technology (MOST). H.-J. W., K.-S. C., and M.-J. L. are also sponsored by the Ministry of Education and Human Resources Development (MOE and HRD) of Korea through the BK21 program.

[1] M. Kwon, J. G. Bak, K. K. Choh, J. H. Choi, J. J. Choi, J. W. Choi, K. S. Chung, Y. S. Chung, A. C. England, J. S. Hong, H. G. Jhang, B. C. Kim, J. Y. Kim, S. S. Kim, W. C. Kim, M. C. Kyum, W. H. Ko, B. J. Lee, D. K. Lee, H. G. Lee, S. G. Lee, T. H. Lho, H. K. Na, B. H. Park, D. C. Seo, S. H. Seo, H. R. Yang, S. J. Yoo, K. I. You, and N. S. Yoon, Nucl. Fusion **43**, 686 (2003).
[2] T. D. Rognlien and M. E. Rensink, Contrib. Plasma Phys. **42**, 193 (2004).
[3] L. Schmitz, B. Merriman, L. Blush, R. Lehmer, R. W. Conn, R. Doerner, A. Grossman, and F. Najmabadi, Phys. Plasmas **2**, 3081 (1995).
[4] T. Ishijima, H. Kubo, M. Shimada, S. Konoshima, S. Higashijima, N. Hosogane, A. Sakasai, K. Itami, T. Sugie, and The JT-60 Team, Plasma Phys. Controlled Fusion **41**, 1155 (1999).
[5] X. Sun, A. M. Keesee, C. Biloiu, E. E. Scime, A. Meige, C. Charles, and R. Boswell, Phys. Rev. Lett. **95**, 025004 (2005).
[6] F. R. Chang-Diaz, Sci. Am. **283**(5), 90 (2000).
[7] A. V. Arefiev and B. N. Breizman, Phys. Plasmas **11**, 2942 (2004).
[8] A. V. Arefiev and B. N. Breizman, Phys. Plasmas **12**, 043504 (2005).
[9] R. L. Stenzel, J. M. Urrutia, M. Griskey, and K. Strohmaier, Phys. Plasmas **9**, 1925 (2002).
[10] W. Gekelman, R. L. Stenzel, and N. Wild, Phys. Scr., T **2**, 177 (1982).
[11] W. Gekelman, S. Vincena, D. Leneman, and J. Maggs, J. Geophys. Res. **102**, 7225 (1997).
[12] K.-S. Chung, H.-J. Woo, G.-S. Choi, J.-J. Do, Y.-J. Seo, and H.-J. You, Contrib. Plasma Phys. **46**, 354 (2006).
[13] D. M. Goebel, J. T. Crow, and A. T. Forrester, Rev. Sci. Instrum. **49**, 469 (1978).
[14] Y. Hirooka, R. W. Conn, T. Sketchley, W. K. Leung, G. Chevalier, R. Doerner, J. Elverum, D. M. Goebel, G. Gunner, M. Khandagle, B. Labombard, R. Lehmer, P. Luong, Y. Ra, L. Schmitz, and G. Tynan, J. Vac. Sci. Technol. A **8**, 1790 (1990).
[15] B. Koch, Ph.D dissertation, Humboldt University, 2004.
[16] N. Ohno, D. Nishijima, S. Takamura, Y. Uesugi, M. Motoyama, N. Hattori, H. Arakawa, N. Ezumi, S. Krasheninnikov, A. Pigarov, and U. Wenzel, Nucl. Fusion **41**, 1055 (2001).
[17] M. Ono, A. Tonegawa, K. Kumita, T. Shibuya, and K. Kawamura, J. Nucl. Mater. **337–339**, 261 (2005).
[18] S. Kado, H. Kobayashi, T. Oishi, and S. Tanaka, J. Nucl. Mater. **313–316**, 754 (2003).
[19] C. Watts, Rev. Sci. Instrum. **75**, 1975 (2004).
[20] F. P. Incropera and D. P. DeWitt, *Fundamentals of Heat and Mass Transfer*, 4th ed (Wiley, New York, 1996) Chap. 12–13.
[21] B. Noyes, Jr., Phys. Rev. **24**, 190 (1924).
[22] Y. H. Jung, J.-S. Yoon, S. J. Yoo, Y.-W. Kim, T. Lho, B. Lee, J.-J. Do, H.-J. Woo, and K.-S. Chung, Contrib. Plasma Phys. **5–6**, 460 (2006).